Acta Cryst E CRYSTALLOGRAPHIC COMMUNICATIONS
ISSN 2056-9890

Synthesis, crystal structure at 219 K and Hirshfeld surface analyses of 1,4,6-trimethylquinoxaline-2,3(1*H*,4*H*)-dione monohydrate

Ayman Zouitini,[a] Md. Serajul Haque Faizi,[b] Younes Ouzidan,[c] Fouad Ouazzani Chahdi,[a] Jérôme Marrot,[d] Damien Prim,[d] Necmi Dege[e] and Ashraf Mashrai[f]*

[a]Laboratoire de Chimie Organique Appliquée, Université Sidi Mohamed Ben Abdallah, Faculté des Sciences et Techniques, BP 2202, Fez, Morocco, [b]Department of Chemistry, Langat Singh College, B.R.A. Bihar University, Muzaffarpur, Bihar-842001, India, [c]Laboratoire de Chimie Physique et Chimie Bio-organique, Faculté des Sciences et Techniques Mohammedia, Université Hassan II, Casablanca, BP 146, 28800, Mohammedia, Morocco, [d]Institut Lavoisier de Versailles, UVSQ, CNRS, Université Paris-Saclay, 78035 Versailles, France, [e]Department of Physics, Faculty of Arts and Sciences, Ondokuz Mayıs University, Samsun, 55200, Turkey, and [f]Department of Pharmacy, University of Science and Technology, Ibb Branch, Ibb, Yemen. *Correspondence e-mail: ashraf.yemen7@gmail.com

Received 17 June 2020
Accepted 13 July 2020

Edited by A. V. Yatsenko, Moscow State University, Russia

Keywords: crystal structure; quinoxaline-2,3-dione; Hirshfeld surface analysis; disorder; hydrogen bonding.

CCDC reference: 1936663

Supporting information: this article has supporting information at journals.iucr.org/e

The asymmetric unit of the title compound, $C_{11}H_{12}N_2O_2\cdot H_2O$, contains a molecule of 1,4,6-trimethyl-1,4-dihydroquinoxaline-2,3-dione and a solvent water molecule. Four atoms of the benzene ring are disordered over two sets of sites in a 0.706 (7):0.294 (7) ratio while the N-bound methyl groups are rotationally disordered with occupancy ratios of 0.78 (4):0.22 (4) and 0.76 (5):0.24 (5). In the crystal, molecules are linked by O—H···O and C—H···O hydrogen bonds into layers lying parallel to $(10\bar{1})$. The Hirshfeld surface analysis indicates that the most important contributions to the packing arrangement are due to H···H (51.3%) and O···H/H···O (28.6%) interactions. The molecular structure calculated by density functional theory is compared with the experimentally determined molecular structure, and the HOMO–LUMO energy gap has been calculated.

1. Chemical context

Quinoxalines are well-known important nitrogen-containing heterocyclic compounds with fused benzene and pyrazine rings. Quinoxalines and their derivatives display various pharmacological and biological activities, such as anticancer (Carta *et al.*, 2006), antidiabetic (Bahekar *et al.*, 2007), antiviral (Fonseca *et al.*, 2004), antibacterial (El-Sabbagh *et al.*, 2009), anti-inflammatory (Wagle *et al.*, 2008) and antiprotozoal (Hui *et al.*, 2006). The present work is a part of an ongoing structural study of quinoxaline derivatives (Faizi & Parashchenko 2015; Faizi *et al.*, 2015, 2018).

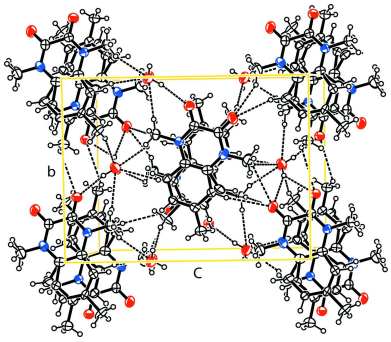

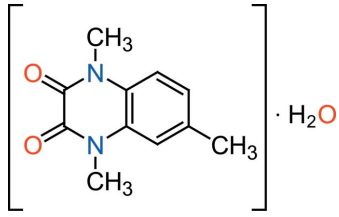

As a continuation of our research devoted to the synthesis and applications of new heterocyclic compounds obtained by *N*-alkylation reactions (Tribak *et al.*, 2017; Qachchachi *et al.*, 2016; Belaziz *et al.*, 2012), we report here the synthesis of 1,4,6-trimethylquinoxaline-2,3(1*H*,4*H*)-dione obtained by the action of iodomethane on 6-methylquinoxaline-2,3(1*H*,4*H*)-dione, and the crystal structure of its monohydrate derivative

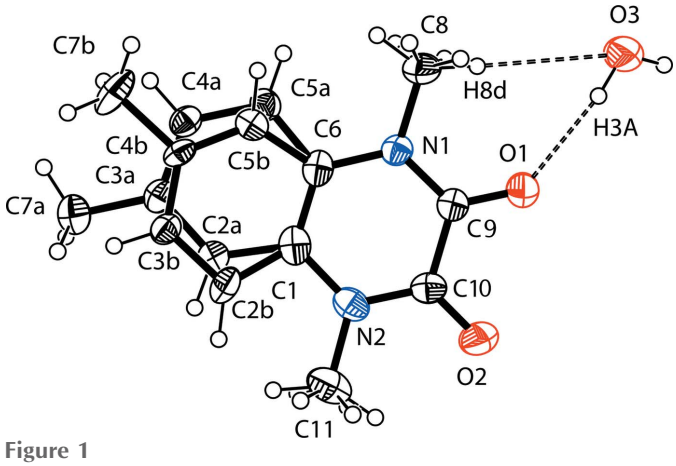

Figure 1
The asymmetric unit of the title compound, showing the atom labelling and displacement ellipsoids drawn at the 40% probability level. O—H···O hydrogen bonds are indicated by dashed lines. The benzene fragment of the organic molecule, C2/C3/C4/C5/C7, is disordered over two sets of sites.

along with the Hirshfeld surface analysis. The experimentally determined molecular structure is compared with that calculated at the DFT/B3LYP/6-311 G(d,p) level.

2. Structural commentary

The title compound crystallizes in space group $P2_1/n$ with one quinoxaline and one water molecule per asymmetric unit. The organic molecule is disordered over two sets of sites with an occupancy ratio of 0.706 (7):0.294 (7). The disorder involves not only the orientation of the methyl group attached to the benzene ring, but also the positions of four carbon atoms of this ring, which are split (Fig. 1). Only the predominant orientation of the 1,4,6-trimethylquinoxaline-2,3(1*H*,4*H*)-dione molecule is discussed below. Besides this, the methyl groups attached to N1 and N2 nitrogen atoms are also rotationally disordered with occupancy ratios of 0.78 (4):0.22 (4) and 0.76 (5):0.24 (5), respectively. The quinoxaline ring system is essentially planar, the largest deviation from the mean plane being 0.015 (3) Å for the N2 atom. The C═O and Csp^2—N bond lengths are typical of such type of compounds and indicate strong conjugation in the amide fragments.

Table 1
Hydrogen-bond geometry (Å, °).

D—H···A	D—H	H···A	D···A	D—H···A
O3—H3*A*···O1	0.86	2.09	2.936 (4)	170
O3—H3*C*···O1^{i}	0.86	2.38	3.062 (4)	137
O3—H3*C*···O2^{i}	0.86	2.19	2.972 (5)	150
C5*A*—H5*A*···O3^{ii}	0.94	2.40	3.298 (13)	160
C8—H8*E*···O2^{iii}	0.97	2.45	3.335 (4)	151

Symmetry codes: (i) $-x+1, -y+3, -z$; (ii) $-x+\frac{1}{2}, y-\frac{1}{2}, -z-\frac{1}{2}$; (iii) $x-\frac{1}{2}, -y+\frac{5}{2}, z-\frac{1}{2}$.

3. Supramolecular features

In the crystal, molecules are linked by O—H···O and C—H···O hydrogen bonds (Table 1) into double layers lying parallel to $(10\bar{1})$. The smallest element of the hydrogen-bonding motif, where the $R_4^2(8)$ rings are formed, is shown in Fig. 2, whereas the whole packing diagram is presented in Fig. 3. The water molecule behaves both as a donor and an acceptor of hydrogen atoms in the hydrogen bonds. As seen in Fig. 3, in centrosymmetric pairs of organic molecules, the aromatic and heterocyclic rings overlap with each other with an intercentroid distance of 3.522 (4) Å, indicating that some π–π interactions occur.

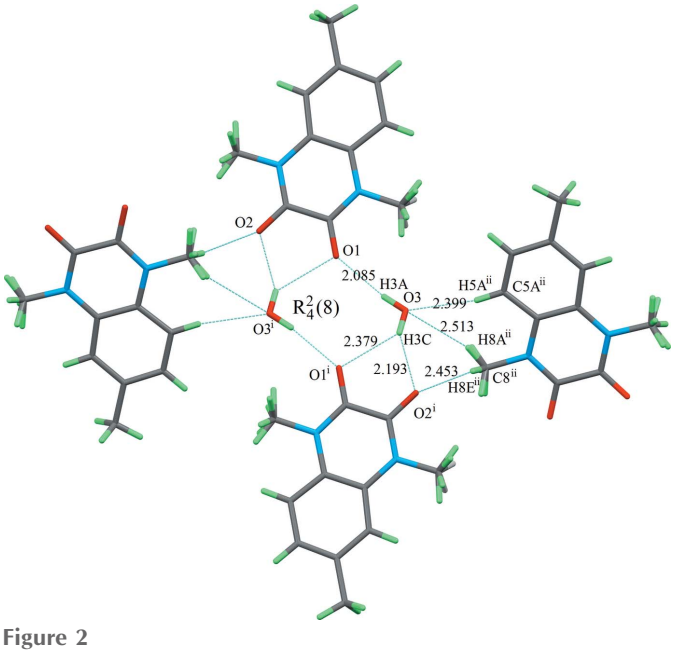

Figure 2
A view along the *a* axis of a hydrogen-bonded fragment. The O—H···O and C—H···O hydrogen bonds (shown as dashed lines) form an $R_4^2(8)$ ring motif.

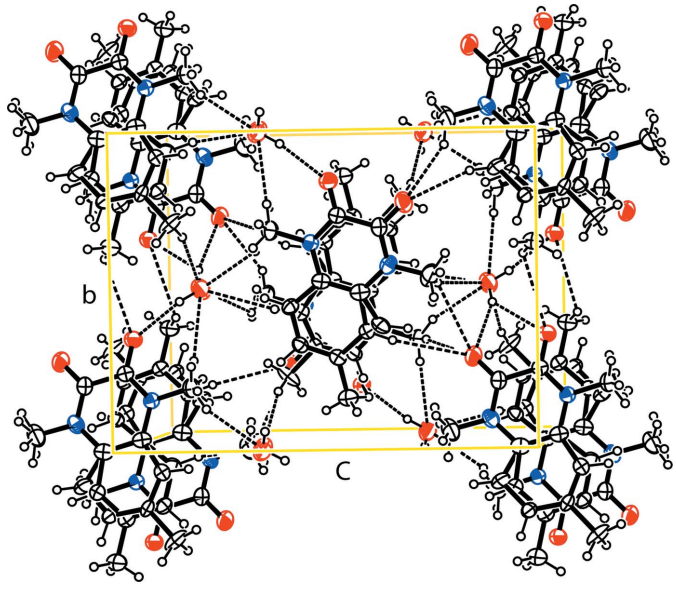

Figure 3
Packing diagram of the title compound viewed along the *a*-axis direction. Only the major disorder component is shown.

4. Hirshfeld surface analysis

The intermolecular interactions were investigated quantitatively and visualized with *Crystal Explorer 17.5* (Turner *et al.*, 2017; Spackman *et al.*, 2009). The d_{norm}, water interaction, curvedness and 2D finger print plots are depicted in Fig. 4*a–c* and 5*a–h*, respectively. The red spots on the Hirshfeld surface represent O—H···O contacts while the blue regions correspond to weak interactions such as C—H···O contacts. The H···H interactions (51.3%) are the major factor in the crystal packing with O···H/H···O interactions (28.6%) representing the next highest contribution. The percentage contributions of other weak interactions are: C···C (8.2%), C···H/H···C (5.8%), C···N/N···C (4.5%), N···H/H···N (1.1%) and O···C/C···O (0.5%).

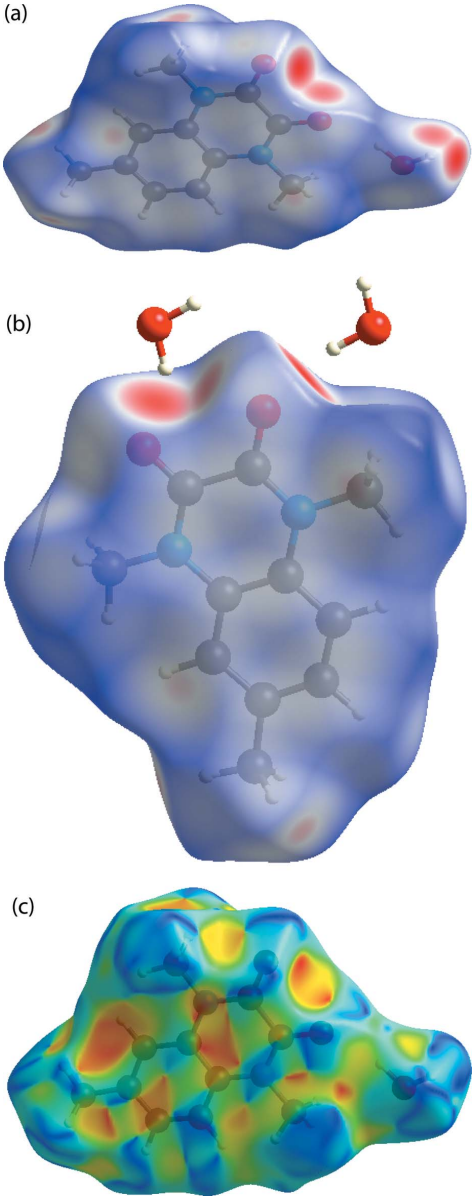

Figure 4
Views of the three-dimensional Hirshfeld surface for the title compound plotted over (*a*, *b*) d_{norm} and (*c*) shape-index.

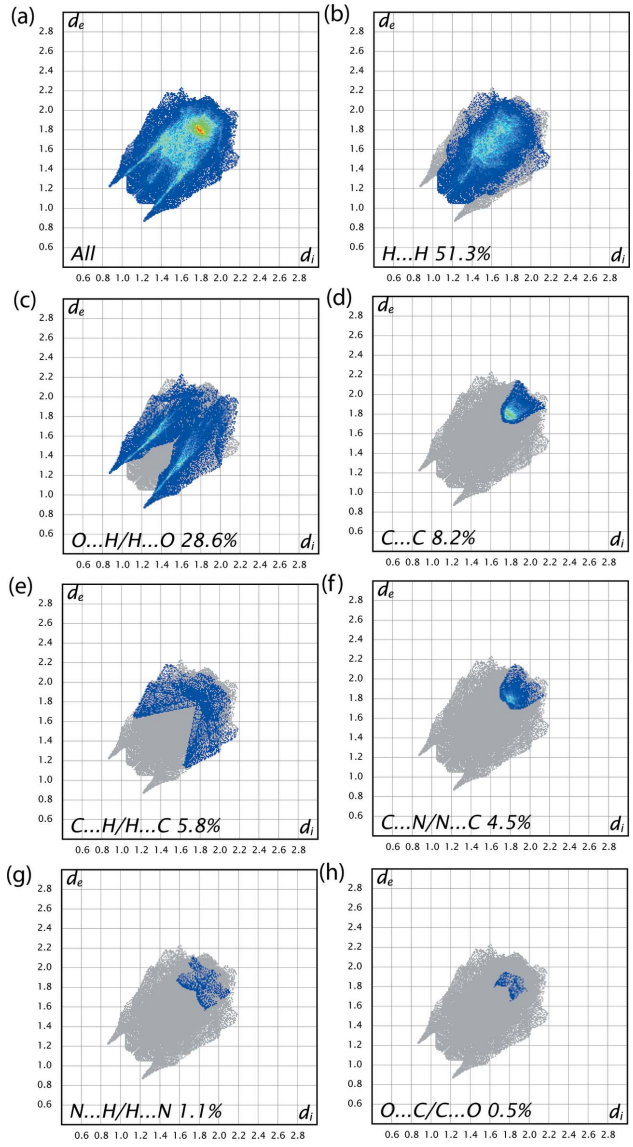

Figure 5
Two-dimensional fingerprint plots showing (*a*) all interactions and those delineated into (*b*) H···H, (*c*) O···H/H···O, (*d*) C···C, (*e*) C···H/H···C, (*f*) C···N/N···C,(*g*) N···H/H···N and (*h*) O···C/C···O.

5. DFT calculations

The structure of the title organic molecule was optimized in the gas-phase approximation at the level of density functional theory (DFT) using the B3LYP functional (Becke, 1993) and 6-311 G(d,p) basis set as implemented in *GAUSSIAN 09* (Frisch *et al.*, 2009). The theoretical and experimental bond lengths and angles are in good agreement (Table 2). The energetic and spatial characteristics of the highest occupied molecular orbital (HOMO), acting as an electron donor, and the lowest unoccupied molecular orbital (LUMO), acting as an electron acceptor, are very important parameters for quantum chemistry. When the energy gap is small, the molecule is highly polarizable and has high chemical reactivity (Fukui, 1982; Khan *et al.*, 2015). The DFT calculations provide

Table 2
Comparison of observed (X-ray data) and calculated (DFT) geometric parameters (Å, °).

Parameter	X-ray	B3LYP/6–311G(d,p)
O1—C9	1.228 (4)	1.217
O2—C10	1.226 (4)	1.211
N1—C6	1.401 (4)	1.407
N1—C8	1.470 (4)	1.468
N1—C9	1.351 (4)	1.375
N2—C1	1.409 (4)	1.375
N2—C10	1.365 (5)	1.384
N2—C11	1.458 (5)	1.464
O1—C9—N1	123.5 (3)	123.9
O2—C10—N2	122.8 (3)	123.4
O1—C9—C10	118.3 (3)	118.3

Table 3
DFT-calculated molecular characteristics for the title compound.

Total Energy, *TE* (eV)	−20757.4747
E_{HOMO} (eV)	−6.1139
E_{LUMO} (eV)	−1.4232
Gap, ΔE (eV)	4.6907
Dipole moment, μ (D)	5.56
Ionization potential, I (eV)	6.1139
Electron affinity, A (eV)	1.4232
Electronegativity, χ	3.929
Hardness, η	2.345
Electrophilicity index, ω	3.291
Softness, σ	0.213
Fraction of electron transferred, ΔN	0.655

some important information on the reactivity and site selectivity of the molecular framework, E_{HOMO} and E_{LUMO}, electronegativity (χ), hardness (η), electrophilicity (ω), softness (σ) and fraction of electrons transferred (ΔN). These data are given in Table 3. The parameters η and σ are significant for evaluation of both the reactivity and stability. The electron transition from HOMO to LUMO is shown in Fig. 6. The HOMO and LUMO are localized in the plane of the whole 1,4,6-trimethylquinoxaline-2,3(1*H*,4*H*)-dione bicyclic ring system. The energy gap [$\Delta E = E_{LUMO} - E_{HOMO}$] of the molecule is 4.6907 eV, the frontier molecular orbital energies E_{HOMO} and E_{LUMO} being −6.1139 eV and −1.4232 eV, respectively. The dipole moment of (I) is estimated to be 5.56 Debye.

6. Database survey

A search of the Cambridge Structural Database (CSD, version 5.39; Groom *et al.*, 2016) gave nine hits for the 1,4,6-trimethylquinoxaline-2,3(1*H*,4*H*)-dione moiety. Two of them are metal complexes, bis(μ_2-nitrato-*O*,*O*,*O*′)-bis[1,4-bis(*N*,*N*-diisopropyl-acetamido)quinoxaline-2,3-dione-*O*,*O*′]tetrakis(nitrato-*O*,*O*′)diaquadineodymium(III) monohydrate (WIKSOZ; Song *et al.*, 2007) and *catena*-(μ_2-iodo)-bis(1,4-dimethylquinoxalin-2,3-dionato)potassium (FADQOS; Benali *et al.*, 2008). Seven organic compounds similar to the title compound are reported in the literature. In 1,4-dihexyl-1,4-dihydroquinoxaline-2,3-dione (FECROX; El Bourakadi *et al.*, 2017*a*), the methyl groups attached to the N atoms are replaced by hexyl groups. In 1,4-diallylquinoxaline-2,3(1*H*,4*H*)-dione (GURGAB; Mustaphi *et al.*, 2001), the allyl groups are bound to the N atoms. In 1-ethyl-4-phenylethyl-1,4-dihydroquinoxaline-2,3-dione (IXATOQ; Akkurt *et al.*, 2004), one N atom is bound to an ethyl group, and the other to an ethylphenyl group. In 6-methyl-1,4-bis[(pyridin-2-yl)methyl]-1,4-dihydroquinoxaline-2,3-dione (KELMIA; Zouitini *et al.*, 2017), methylpyridinyl groups are attached to both N atoms. In 1,4-dibenzyl-6-chloro-1,4-dihydroquinoxaline-2,3-dione (PAWFEB; El Janati *et al.*, 2017*a*), the N atoms are attached to the benzyl groups, and the methyl group on the benzene ring is substituted by chlorine. In 1,4-dioctyl-1,4-dihydroquinoxaline-2,3-dione (WAPWAO; El Bourakadi *et al.*, 2017*b*), octyl groups are attached to the N atoms. In 6-chloro-1,4-diethyl-1,4-dihydroquinoxaline-2,3-dione (XEFMON; El Janati *et al.*, 2017*b*), the ethyl groups are attached to the N atoms, and the methyl group on the benzene ring is substituted by chlorine, as in PAWFEB. None of these structures contains solvent molecules.

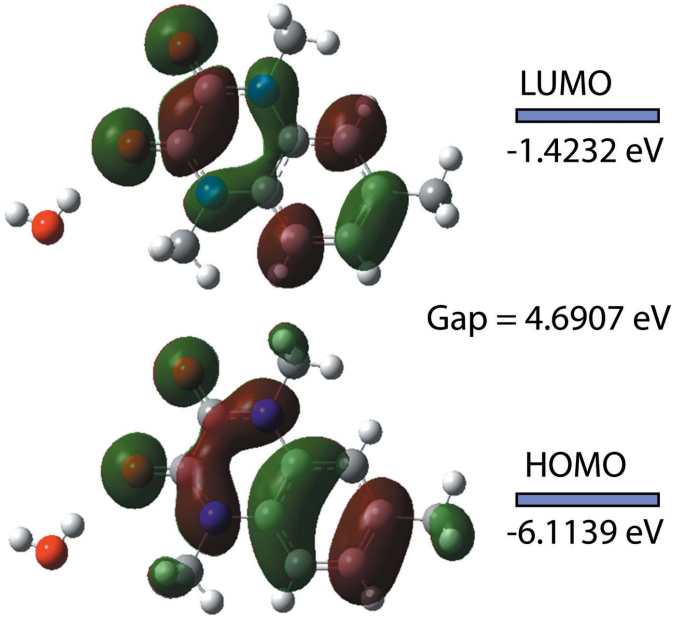

Figure 6
Frontier molecular orbitals of the 1,4,6-trimethylquinoxaline-2,3(1*H*,4*H*)-dione molecule.

7. Synthesis and crystallization

To a solution of 6-methyl-1,4-dihydroquinoxaline-2,3-dione (0.3 g, 1.73 mmol) in DMF (15 ml) potassium carbonate (0.47 g, 3.61 mmol) and tetra-*n*-butylammonium (0.07g, 0.23 mmol) were added. After 10 min of stirring, 0.27 ml (4.32 mmol) of iodomethane were added, and the mixture was stirred at room temperature for 6 h. The inorganic salts were filtered off, DMF was evaporated under reduced pressure and the residue was dissolved in dichloromethane. The organic phase was dried over Na_2SO_4 and then concentrated. The crude product was purified by chromatography on a silica gel column [eluent: hexane/ethylacetate (2/1)].

Table 4
Experimental details.

Crystal data	
Chemical formula	$C_{11}H_{12}N_2O_2{\cdot}H_2O$
M_r	222.24
Crystal system, space group	Monoclinic, $P2_1/n$
Temperature (K)	219
a, b, c (Å)	7.0695 (4), 10.8321 (5), 14.4349 (6)
β (°)	101.556 (3)
V (Å^3)	1082.98 (9)
Z	4
Radiation type	Mo $K\alpha$
μ (mm^{-1})	0.10
Crystal size (mm)	0.30 × 0.18 × 0.04
Data collection	
Diffractometer	Bruker APEXII CCD
Absorption correction	Multi-scan (*SADABS*; Krause *et al.*, 2015)
No. of measured, independent and observed [$I > 2\sigma(I)$] reflections	32798, 1935, 1563
R_{int}	0.062
(sin $\theta/\lambda)_{max}$ (Å^{-1})	0.598
Refinement	
$R[F^2 > 2\sigma(F^2)]$, $wR(F^2)$, S	0.067, 0.147, 1.24
No. of reflections	1935
No. of parameters	201
No. of restraints	30
H-atom treatment	H-atom parameters constrained
$\Delta\rho_{max}$, $\Delta\rho_{min}$ (e Å^{-3})	0.21, −0.18

Computer programs: *APEX3* and *SAINT* (Bruker, 2016), *SHELXT* (Sheldrick, 2015*a*), *SHELXL2018* (Sheldrick, 2015*b*), *OLEX2* (Dolomanov *et al.*, 2009), *Mercury* (Macrae *et al.*, 2020), *WinGX* (Farrugia, 2012), *PLATON* (Spek, 2020) and *publCIF* (Westrip, 2010).

8. Refinement

Crystal data, data collection and structure refinement details are summarized in Table 4. Water molecules were refined as rigid groups with U_{iso}(H) = 1.5U_{eq}(O). Other H atoms were positioned geometrically, with C—H = 0.94 and 0.97 Å for aromatic and aliphatic H atoms, respectively, and constrained to ride on their parent atoms, with U_{iso}(H) = 1.2U_{eq}(C) or U_{iso}(H) = 1.5U_{eq}(C-methyl). The disorder of the organic molecule was taken into account using free variables.

Acknowledgements

Langat Singh College, B·R. Bihar University India is thanked for access to laboratory facilities.

Funding information

Funding for this research was provided by: University Grants Commission, New Delhi. This study was supported financially by Université Sidi Mohamed Ben Abdallah, Faculté des Sciences et Techniques, Morocco and the University of Science and Technology, Ibb Branch, Ibb, Yemen.

References

Akkurt, M., Öztürk, S., Küçükbay, H., Orhan, E. & Büyükgüngör, O. (2004). *Acta Cryst.* E**60**, o1266–o1268.
Bahekar, R. H., Jain, M. R., Gupta, A. A., Goel, A., Jadav, P. A., Patel, D. N., Prajapati, V. M. & Patel, P. R. (2007). *Arch. Pharm. Chem. Life Sci.* **340**, 359–366.
Becke, A. D. (1993). *J. Chem. Phys.* **98**, 5648–5652.
Belaziz, D., Kandri Rodi, Y., Essassi, E. M. & El Ammari, L. (2012). *Acta Cryst.* E**68**, o1276.
Benali, B., Lazar, Z., Boucetta, A., El Assyry, A., Lakhrissi, B., Massoui, M., Jermoumi, C., Negrier, P., Leger, J. M. & Mondieig, D. (2008). *Spectrosc. Lett.* **41**, 64–71.
Bruker (2016). *APEX3* and *SAINT*. Bruker AXS Inc., Madison, Wisconsin, USA.
Carta, A., Loriga, M., Piras, S., Paglietti, G., La Colla, P., Busonera, B., Collu, G. & Loddo, R. (2006). *Med. Chem.* **2**, 113–122.
Dolomanov, O. V., Bourhis, L. J., Gildea, R. J., Howard, J. A. K. & Puschmann, H. (2009). *J. Appl. Cryst.* **42**, 339–341.
El Bourakadi, K., El Bakri, Y., Sebhaoui, J., Rayni, I., Essassi, E. M. & Mague, J. T. (2017*a*). *IUCrData*, **2**, x171019.
El Bourakadi, K., El Bakri, Y., Sebhaoui, J., Rayni, I., Essassi, E. M. & Mague, J. T. (2017*b*). *IUCrData*, **2**, x170520.
El Janati, A., Kandri Rodi, Y., Jasinski, J. P., Kaur, M., Ouzidan, Y. & Essassi, E. M. (2017*a*). *IUCrData*, **2**, x170901.
El Janati, A., Kandri Rodi, Y., Jasinski, J. P., Kaur, M., Ouzidan, Y. & Essassi, E. M. (2017*b*). *IUCrData*, **2**, x171052.
El-Sabbagh, O. I., El-Sadek, M. E., Lashine, S. M., Yassin, S. H. & El-Nabtity, S. M. (2009). *Med. Chem. Res.* **18**, 782–797.
Faizi, M. S. H., Alam, M. J., Haque, A., Ahmad, S., Shahid, M. & Ahmad, M. (2018). *J. Mol. Struct.* **1156**, 457–464.
Faizi, M. S. H. & Parashchenko, Y. (2015). *Acta Cryst.* E**71**, 1332–1335.
Faizi, M. S. H., Sharkina, N. O. & Iskenderov, T. S. (2015). *Acta Cryst.* E**71**, o17–o18.
Farrugia, L. J. (2012). *J. Appl. Cryst.* **45**, 849–854.
Fonseca, T., Gigante, B., Marques, M. M., Gilchrist, T. L. & De Clercq, E. (2004). *Bioorg. Med. Chem.* **12**, 103–112.
Frisch, M. J., Trucks, G. W., Schlegel, H. B., Scuseria, G. E., Robb, M. A., Cheeseman, J. R., Scalmani, G., Barone, V., Mennucci, B., Petersson, G. A., Nakatsuji, H., Caricato, M., Li, X., Hratchian, H. P., Izmaylov, A. F., Bloino, J., Zheng, G., Sonnenberg, J. L., Hada, M., Ehara, M., Toyota, K., Fukuda, R., Hasegawa, J., Ishida, M., Nakajima, T., Honda, Y., Kitao, O., Nakai, H., Vreven, T., Montgomery, J. A. Jr, Peralta, J. E., Ogliaro, F., Bearpark, M., Heyd, J. J., Brothers, E., Kudin, K. N., Staroverov, V. N., Kobayashi, R., Normand, J., Raghavachari, K., Rendell, A., Burant, J. C., Iyengar, S. S., Tomasi, J., Cossi, M., Rega, N., Millam, J. M., Klene, M., Knox, J. E., Cross, J. B., Bakken, V., Adamo, C., Jaramillo, J., Gomperts, R., Stratmann, R. E., Yazyev, O., Austin, A. J., Cammi, R., Pomelli, C., Ochterski, J. W., Martin, R. L., Morokuma, K., Zakrzewski, V. G., Voth, G. A., Salvador, P., Dannenberg, J. J., Dapprich, S., Daniels, A. D., Farkas, Ö., Foresman, J. B., Ortiz, J. V., Cioslowski, J. & Fox, D. J. (2009). *GAUSSIAN09*. Gaussian Inc., Wallingford, CT, USA.
Fukui, K. (1982). *Science*, **218**, 747–754.
Groom, C. R., Bruno, I. J., Lightfoot, M. P. & Ward, S. C. (2016). *Acta Cryst.* B**72**, 171–179.
Hui, X., Desrivot, J., Bories, C., Loiseau, P. M., Franck, X., Hocquemiller, R. & Figadère, B. (2006). *Bioorg. Med. Chem. Lett.* **16**, 815–820.
Khan, E., Shukla, A., Srivastava, A., Shweta, P. & Tandon, P. (2015). *New J. Chem.* **39**, 9800–9812.
Krause, L., Herbst-Irmer, R., Sheldrick, G. M. & Stalke, D. (2015). *J. Appl. Cryst.* **48**, 3–10.
Macrae, C. F., Sovago, I., Cottrell, S. J., Galek, P. T. A., McCabe, P., Pidcock, E., Platings, M., Shields, G. P., Stevens, J. S., Towler, M. & Wood, P. A. (2020). *J. Appl. Cryst.* **53**, 226–235.
Mustaphi, N. E., Ferfra, S., Essassi, E. M. & Pierrot, M. (2001). *Acta Cryst.* E**57**, o176–o177.
Qachchachi, F., Kandri Rodi, Y., Elmsellem, H., Steli, H., Haoudi, A., Mazzah, A., Ouzidan, Y., Sebbar, N. K. & Essassi, E. M. (2016). *J. Materials Environ. Sci.* **7**, 2897–2907.
Sheldrick, G. M. (2015*a*). *Acta Cryst.* A**71**, 3–8.
Sheldrick, G. M. (2015*b*). *Acta Cryst.* C**71**, 3–8.

Song, X.-Q., Yu, Y., Liu, W.-S., Dou, W., Zheng, J.-R. & Yao, J.-N. (2007). *J. Solid State Chem.* **180**, 2616–2624.
Spackman, M. A. & Jayatilaka, D. (2009). *CrystEngComm*, **11**, 19–32.
Spek, A. L. (2020). *Acta Cryst.* E**76**, 1–11.
Tribak, Z., Kandri Rodi, Y., Haoudi, A., Skalli, M. K., Mazzah, A., Akhazzane, M. & Essassi, E. M. (2017). *J. Mar. Chim. Heterocycl.* **16**, 58–65.
Turner, M. J., Mckinnon, J. J., Wolff, S. K., Grimwood, D. J., Spackman, P. R., Jayatilaka, D. & Spackman, M. A. (2017). *Crystal Explorer 17.5*. The University of Western Australia.
Wagle, S., Adhikari, A. V. & Kumari, N. S. (2008). *Indian J. Chem.* **47**, 439–448.
Westrip, S. P. (2010). *J. Appl. Cryst.* **43**, 920–925.
Zouitini, A., Kandri Rodi, Y., Ouazzani Chahdi, F., Jasinski, J. P., Kaur, M. & Essassi, E. M. (2017). *IUCrData*, **2**, x171651.

supporting information

Acta Cryst. (2020). E**76**, 1296-1301 [https://doi.org/10.1107/S2056989020009573]

Synthesis, crystal structure at 219 K and Hirshfeld surface analyses of 1,4,6-trimethylquinoxaline-2,3(1*H*,4*H*)-dione monohydrate

Ayman Zouitini, Md. Serajul Haque Faizi, Younes Ouzidan, Fouad Ouazzani Chahdi, Jérôme Marrot, Damien Prim, Necmi Dege and Ashraf Mashrai

Computing details

Data collection: *APEX3* (Bruker, 2016); cell refinement: *SAINT* (Bruker, 2016); data reduction: *SAINT* (Bruker, 2016); program(s) used to solve structure: SHELXT (Sheldrick, 2015a); program(s) used to refine structure: *SHELXL2018* (Sheldrick, 2015b); molecular graphics: *OLEX2* (Dolomanov *et al.*, 2009) and *Mercury* (Macrae *et al.*, 2020); software used to prepare material for publication: *WinGX* (Farrugia, 2012), *PLATON* (Spek, 2020) and *publCIF* (Westrip, 2010).

1,4,6-Trimethylquinoxaline-2,3(1*H*,4*H*)-dione monohydrate

Crystal data

$C_{11}H_{12}N_2O_2{\cdot}H_2O$
M_r = 222.24
Monoclinic, $P2_1/n$
a = 7.0695 (4) Å
b = 10.8321 (5) Å
c = 14.4349 (6) Å
β = 101.556 (3)°
V = 1082.98 (9) Å^3
Z = 4
$F(000)$ = 472
D_x = 1.363 Mg m^{-3}
Mo $K\alpha$ radiation, λ = 0.71073 Å
Cell parameters from 7373 reflections
θ = 2.4–24.7°
μ = 0.10 mm^{-1}
T = 219 K
Parallelepiped, yellow
0.30 × 0.18 × 0.04 mm

Data collection

Bruker APEXII CCD diffractometer
Radiation source: fine-focus sealed tube
φ and ω scans
Absorption correction: multi-scan (SADABS; Krause *et al.*, 2015)
32798 measured reflections
1935 independent reflections
1563 reflections with $I > 2\sigma(I)$
R_{int} = 0.062
θ_{max} = 25.2°, θ_{min} = 2.4°
h = −8→8
k = −12→12
l = −17→17

Refinement

Refinement on F^2
Least-squares matrix: full
$R[F^2 > 2\sigma(F^2)]$ = 0.067
$wR(F^2)$ = 0.147
S = 1.24
1935 reflections
201 parameters
30 restraints
Primary atom site location: structure-invariant direct methods
Secondary atom site location: difference Fourier map
Hydrogen site location: mixed
H-atom parameters constrained
$w = 1/[\sigma^2(F_o^2) + (0.0097P)^2 + 1.8308P]$ where $P = (F_o^2 + 2F_c^2)/3$
$(\Delta/\sigma)_{max} < 0.001$

$\Delta\rho_{max}$ = 0.21 e Å^{-3}
$\Delta\rho_{min}$ = −0.18 e Å^{-3}

Extinction correction: SHELXL2018 (Sheldrick, 2015b), $Fc^*=kFc[1+0.001xFc^2\lambda^3/\sin(2\theta)]^{-1/4}$
Extinction coefficient: 0.0031 (9)

Special details

Geometry. All esds (except the esd in the dihedral angle between two l.s. planes) are estimated using the full covariance matrix. The cell esds are taken into account individually in the estimation of esds in distances, angles and torsion angles; correlations between esds in cell parameters are only used when they are defined by crystal symmetry. An approximate (isotropic) treatment of cell esds is used for estimating esds involving l.s. planes.

Fractional atomic coordinates and isotropic or equivalent isotropic displacement parameters (Å^2)

	x	*y*	*z*	U_{iso}*/U_{eq}	Occ. (<1)
O1	0.3712 (4)	1.3409 (2)	0.00205 (17)	0.0479 (7)	
O2	0.3853 (4)	1.2710 (3)	0.18106 (17)	0.0581 (8)	
C1	0.2612 (4)	0.9861 (3)	0.0618 (3)	0.0409 (8)	
C2A	0.2177 (14)	0.8598 (10)	0.0725 (6)	0.034 (2)	0.706 (7)
H2A	0.219201	0.830335	0.133895	0.041*	0.706 (7)
C2B	0.228 (5)	0.879 (3)	0.1074 (16)	0.048 (7)	0.294 (7)
H2B	0.237848	0.867991	0.172811	0.057*	0.294 (7)
C3A	0.1723 (13)	0.7756 (12)	−0.0031 (7)	0.037 (2)	0.706 (7)
C3B	0.175 (4)	0.788 (3)	0.0367 (16)	0.037 (5)	0.294 (7)
H3B	0.152151	0.706837	0.055446	0.045*	0.294 (7)
C4A	0.1703 (14)	0.8174 (10)	−0.0933 (6)	0.038 (2)	0.706 (7)
H4A	0.142000	0.761812	−0.144148	0.045*	0.706 (7)
C4B	0.156 (3)	0.811 (2)	−0.0554 (16)	0.035 (6)	0.294 (7)
C5A	0.210 (2)	0.9418 (16)	−0.1111 (9)	0.039 (3)	0.706 (7)
H5A	0.207157	0.970180	−0.172834	0.047*	0.706 (7)
C5B	0.193 (5)	0.923 (4)	−0.087 (2)	0.032 (6)	0.294 (7)
H5B	0.176018	0.933494	−0.153049	0.038*	0.294 (7)
C6	0.2535 (4)	1.0233 (3)	−0.0314 (2)	0.0369 (8)	
N1	0.2915 (4)	1.1465 (2)	−0.05089 (18)	0.0359 (7)	
C9	0.3382 (4)	1.2324 (3)	0.0177 (2)	0.0354 (7)	
C10	0.3472 (5)	1.1936 (3)	0.1182 (2)	0.0402 (8)	
N2	0.3101 (4)	1.0729 (3)	0.1354 (2)	0.0440 (7)	
C8	0.2761 (6)	1.1869 (4)	−0.1493 (2)	0.0540 (10)	
H8A	0.223018	1.120497	−0.191729	0.081*	0.22 (4)
H8B	0.403194	1.208575	−0.159941	0.081*	0.22 (4)
H8C	0.191973	1.258317	−0.161254	0.081*	0.22 (4)
H8D	0.322439	1.271095	−0.150220	0.081*	0.78 (4)
H8E	0.142263	1.183017	−0.182009	0.081*	0.78 (4)
H8F	0.353484	1.133275	−0.180695	0.081*	0.78 (4)
C11	0.3169 (7)	1.0381 (4)	0.2335 (3)	0.0696 (13)	
H11A	0.279949	0.952205	0.236449	0.104*	0.24 (5)
H11B	0.228285	1.089532	0.259797	0.104*	0.24 (5)
H11C	0.446948	1.049549	0.269709	0.104*	0.24 (5)
H11D	0.356839	1.108652	0.274187	0.104*	0.76 (5)
H11E	0.408503	0.971326	0.250839	0.104*	0.76 (5)

H11F	0.189839	1.011308	0.240928	0.104*	0.76 (5)
O3	0.3982 (6)	1.4989 (3)	−0.1600 (2)	0.0833 (11)	
H3A	0.382975	1.460410	−0.109907	0.125*	
H3C	0.477462	1.559146	−0.144450	0.125*	
C7A	0.1315 (8)	0.6428 (5)	0.0165 (4)	0.0528 (17)	0.706 (7)
H7A2	0.035271	0.639039	0.055782	0.079*	0.706 (7)
H7A3	0.249382	0.603381	0.049019	0.079*	0.706 (7)
H7A1	0.083495	0.600399	−0.042761	0.079*	0.706 (7)
C7B	0.0926 (19)	0.7135 (13)	−0.1317 (10)	0.062 (5)	0.294 (7)
H7B1	0.025634	0.753011	−0.189272	0.093*	0.294 (7)
H7B2	0.006626	0.655227	−0.110056	0.093*	0.294 (7)
H7B3	0.205065	0.670198	−0.143967	0.093*	0.294 (7)

Atomic displacement parameters (Å²)

	U^{11}	U^{22}	U^{33}	U^{12}	U^{13}	U^{23}
O1	0.0528 (15)	0.0419 (15)	0.0475 (14)	−0.0027 (12)	0.0067 (11)	0.0004 (12)
O2	0.0675 (18)	0.0632 (18)	0.0414 (14)	−0.0097 (14)	0.0057 (12)	−0.0075 (14)
C1	0.0219 (15)	0.0408 (19)	0.059 (2)	0.0014 (14)	0.0050 (14)	0.0022 (17)
C2A	0.026 (3)	0.038 (6)	0.038 (5)	0.003 (3)	0.007 (4)	0.000 (5)
C2B	0.051 (9)	0.040 (10)	0.051 (13)	−0.009 (7)	0.008 (11)	−0.016 (11)
C3A	0.029 (3)	0.039 (5)	0.043 (8)	−0.003 (3)	0.006 (5)	−0.005 (6)
C3B	0.040 (8)	0.034 (10)	0.036 (13)	0.003 (7)	0.003 (10)	−0.004 (11)
C4A	0.035 (3)	0.039 (4)	0.037 (5)	0.003 (2)	0.002 (4)	−0.005 (4)
C4B	0.033 (7)	0.042 (11)	0.029 (14)	−0.002 (7)	0.008 (10)	−0.013 (11)
C5A	0.038 (5)	0.038 (5)	0.039 (6)	−0.002 (4)	0.002 (4)	0.006 (4)
C5B	0.014 (7)	0.042 (14)	0.038 (13)	0.005 (7)	0.003 (8)	0.005 (10)
C6	0.0200 (15)	0.0367 (18)	0.050 (2)	0.0025 (13)	−0.0020 (13)	−0.0011 (15)
N1	0.0297 (14)	0.0393 (15)	0.0358 (15)	0.0005 (12)	−0.0002 (11)	−0.0006 (12)
C9	0.0259 (16)	0.0385 (19)	0.0407 (18)	0.0022 (14)	0.0037 (13)	−0.0001 (15)
C10	0.0318 (17)	0.052 (2)	0.0362 (18)	−0.0002 (15)	0.0048 (14)	−0.0006 (16)
N2	0.0360 (15)	0.0523 (18)	0.0448 (17)	0.0004 (14)	0.0108 (13)	0.0091 (14)
C8	0.063 (3)	0.057 (2)	0.037 (2)	0.002 (2)	−0.0016 (17)	0.0010 (17)
C11	0.081 (3)	0.078 (3)	0.054 (3)	0.002 (3)	0.023 (2)	0.017 (2)
O3	0.127 (3)	0.069 (2)	0.0480 (17)	−0.041 (2)	0.0053 (18)	0.0030 (16)
C7A	0.055 (3)	0.041 (3)	0.063 (4)	−0.001 (2)	0.013 (3)	0.002 (3)
C7B	0.048 (8)	0.063 (9)	0.077 (10)	−0.005 (7)	0.014 (7)	−0.045 (8)

Geometric parameters (Å, º)

O1—C9	1.228 (4)	N1—C8	1.470 (4)
O2—C10	1.226 (4)	C9—C10	1.499 (5)
C1—C2B	1.38 (3)	C10—N2	1.365 (5)
C1—C6	1.394 (5)	N2—C11	1.458 (5)
C1—N2	1.409 (4)	C8—H8A	0.9700
C1—C2A	1.418 (12)	C8—H8B	0.9700
C2A—C3A	1.409 (11)	C8—H8C	0.9700
C2A—H2A	0.9400	C8—H8D	0.9700

C2B—C3B	1.41 (2)	C8—H8E	0.9700
C2B—H2B	0.9400	C8—H8F	0.9700
C3A—C4A	1.375 (11)	C11—H11A	0.9700
C3A—C7A	1.504 (14)	C11—H11B	0.9700
C3B—C4B	1.34 (3)	C11—H11C	0.9700
C3B—H3B	0.9400	C11—H11D	0.9700
C4A—C5A	1.41 (2)	C11—H11E	0.9700
C4A—H4A	0.9400	C11—H11F	0.9700
C4B—C5B	1.34 (4)	O3—H3A	0.8603
C4B—C7B	1.53 (2)	O3—H3C	0.8598
C5A—C6	1.434 (17)	C7A—H7A2	0.9700
C5A—H5A	0.9400	C7A—H7A3	0.9700
C5B—C6	1.37 (4)	C7A—H7A1	0.9700
C5B—H5B	0.9400	C7B—H7B1	0.9700
C6—N1	1.401 (4)	C7B—H7B2	0.9700
N1—C9	1.351 (4)	C7B—H7B3	0.9700

C2B—C1—C6	136.5 (10)	H8B—C8—H8C	109.5
C2B—C1—N2	104.1 (10)	N1—C8—H8D	109.5
C6—C1—N2	119.4 (3)	H8A—C8—H8D	141.1
C6—C1—C2A	114.6 (5)	H8B—C8—H8D	56.3
N2—C1—C2A	126.0 (5)	H8C—C8—H8D	56.3
C3A—C2A—C1	124.1 (8)	N1—C8—H8E	109.5
C3A—C2A—H2A	117.9	H8A—C8—H8E	56.3
C1—C2A—H2A	117.9	H8B—C8—H8E	141.1
C1—C2B—C3B	107 (2)	H8C—C8—H8E	56.3
C1—C2B—H2B	126.6	H8D—C8—H8E	109.5
C3B—C2B—H2B	126.6	N1—C8—H8F	109.5
C4A—C3A—C2A	118.5 (11)	H8A—C8—H8F	56.3
C4A—C3A—C7A	121.8 (10)	H8B—C8—H8F	56.3
C2A—C3A—C7A	119.7 (9)	H8C—C8—H8F	141.1
C4B—C3B—C2B	123 (3)	H8D—C8—H8F	109.5
C4B—C3B—H3B	118.5	H8E—C8—H8F	109.5
C2B—C3B—H3B	118.5	N2—C11—H11A	109.5
C3A—C4A—C5A	121.5 (11)	N2—C11—H11B	109.5
C3A—C4A—H4A	119.2	H11A—C11—H11B	109.5
C5A—C4A—H4A	119.2	N2—C11—H11C	109.5
C3B—C4B—C5B	122 (3)	H11A—C11—H11C	109.5
C3B—C4B—C7B	123 (2)	H11B—C11—H11C	109.5
C5B—C4B—C7B	115 (2)	N2—C11—H11D	109.5
C4A—C5A—C6	117.4 (9)	H11A—C11—H11D	141.1
C4A—C5A—H5A	121.3	H11B—C11—H11D	56.3
C6—C5A—H5A	121.3	H11C—C11—H11D	56.3
C4B—C5B—C6	125 (2)	N2—C11—H11E	109.5
C4B—C5B—H5B	117.5	H11A—C11—H11E	56.3
C6—C5B—H5B	117.5	H11B—C11—H11E	141.1
C5B—C6—C1	106.7 (11)	H11C—C11—H11E	56.3
C5B—C6—N1	133.4 (11)	H11D—C11—H11E	109.5

C1—C6—N1	119.8 (3)	N2—C11—H11F	109.5
C1—C6—C5A	123.8 (6)	H11A—C11—H11F	56.3
N1—C6—C5A	116.4 (6)	H11B—C11—H11F	56.3
C9—N1—C6	122.5 (3)	H11C—C11—H11F	141.1
C9—N1—C8	117.6 (3)	H11D—C11—H11F	109.5
C6—N1—C8	119.9 (3)	H11E—C11—H11F	109.5
O1—C9—N1	123.5 (3)	H3A—O3—H3C	109.5
O1—C9—C10	118.3 (3)	C3A—C7A—H7A2	109.5
N1—C9—C10	118.2 (3)	C3A—C7A—H7A3	109.5
O2—C10—N2	122.8 (3)	H7A2—C7A—H7A3	109.5
O2—C10—C9	119.0 (3)	C3A—C7A—H7A1	109.5
N2—C10—C9	118.2 (3)	H7A2—C7A—H7A1	109.5
C10—N2—C1	121.9 (3)	H7A3—C7A—H7A1	109.5
C10—N2—C11	117.0 (3)	C4B—C7B—H7B1	109.5
C1—N2—C11	121.0 (3)	C4B—C7B—H7B2	109.5
N1—C8—H8A	109.5	H7B1—C7B—H7B2	109.5
N1—C8—H8B	109.5	C4B—C7B—H7B3	109.5
H8A—C8—H8B	109.5	H7B1—C7B—H7B3	109.5
N1—C8—H8C	109.5	H7B2—C7B—H7B3	109.5
H8A—C8—H8C	109.5		

C6—C1—C2A—C3A	0.8 (11)	C5B—C6—N1—C9	175.2 (19)
N2—C1—C2A—C3A	−179.0 (7)	C1—C6—N1—C9	0.7 (4)
C6—C1—C2B—C3B	1 (4)	C5A—C6—N1—C9	−178.8 (8)
N2—C1—C2B—C3B	179.2 (19)	C5B—C6—N1—C8	−3 (2)
C1—C2A—C3A—C4A	0.2 (15)	C1—C6—N1—C8	−177.6 (3)
C1—C2A—C3A—C7A	179.0 (7)	C5A—C6—N1—C8	2.8 (9)
C1—C2B—C3B—C4B	−3 (4)	C6—N1—C9—O1	−179.7 (3)
C2A—C3A—C4A—C5A	−0.9 (17)	C8—N1—C9—O1	−1.3 (5)
C7A—C3A—C4A—C5A	−179.7 (10)	C6—N1—C9—C10	−0.6 (4)
C2B—C3B—C4B—C5B	2 (5)	C8—N1—C9—C10	177.8 (3)
C2B—C3B—C4B—C7B	−178 (2)	O1—C9—C10—O2	0.6 (5)
C3A—C4A—C5A—C6	0.5 (19)	N1—C9—C10—O2	−178.5 (3)
C3B—C4B—C5B—C6	0 (5)	O1—C9—C10—N2	179.9 (3)
C7B—C4B—C5B—C6	−179 (2)	N1—C9—C10—N2	0.8 (4)
C4B—C5B—C6—C1	−2 (3)	O2—C10—N2—C1	178.2 (3)
C4B—C5B—C6—N1	−177.0 (19)	C9—C10—N2—C1	−1.0 (4)
C2B—C1—C6—C5B	1 (2)	O2—C10—N2—C11	0.1 (5)
N2—C1—C6—C5B	−176.8 (15)	C9—C10—N2—C11	−179.1 (3)
C2B—C1—C6—N1	177.2 (19)	C2B—C1—N2—C10	−177.6 (14)
N2—C1—C6—N1	−0.9 (4)	C6—C1—N2—C10	1.1 (4)
C2A—C1—C6—N1	179.2 (5)	C2A—C1—N2—C10	−179.0 (5)
N2—C1—C6—C5A	178.5 (9)	C2B—C1—N2—C11	0.4 (14)
C2A—C1—C6—C5A	−1.3 (10)	C6—C1—N2—C11	179.1 (3)
C4A—C5A—C6—C1	0.7 (17)	C2A—C1—N2—C11	−1.1 (7)
C4A—C5A—C6—N1	−179.8 (9)		

Hydrogen-bond geometry (Å, º)

D—H···*A*	*D*—H	H···*A*	*D*···*A*	*D*—H···*A*
O3—H3*A*···O1	0.86	2.09	2.936 (4)	170
O3—H3*C*···O1^{i}	0.86	2.38	3.062 (4)	137
O3—H3*C*···O2^{i}	0.86	2.19	2.972 (5)	150
C5*A*—H5*A*···O3^{ii}	0.94	2.40	3.298 (13)	160
C8—H8*E*···O2^{iii}	0.97	2.45	3.335 (4)	151

Symmetry codes: (i) −*x*+1, −*y*+3, −*z*; (ii) −*x*+1/2, *y*−1/2, −*z*−1/2; (iii) *x*−1/2, −*y*+5/2, *z*−1/2.